Magnetic anisotropies of sputtered Fe films on MgO substrates

Yu. V. Goryunov, N. N. Garif'yanov, G. G. Khaliullin, and I. A. Garifullin
Kazan Physicotechnical Institute of Russian Academy of Sciences, 420029 Kazan, Russian Federation

L. R. Tagirov
Kazan State University, 420008 Kazan, Russian Federation

F. Schreiber, Th. Mühge, and H. Zabel
Institut für Experimentalphysik, Fakultät für Physik und Astronomie, Ruhr-Universität Bochum, D-44780 Bochum, Germany
(Received 23 June 1995)

Ferromagnetic resonance (FMR) and superconducting quantum interference device (SQUID) measurements have been used to study the magnetic properties of rf sputtered Fe films on MgO(001) substrates. The dependences of the FMR spectra parameters on the direction of the dc magnetic field turning in the plane of the films were measured in a wide temperature range (20–400 K) for films with thickness L in the range 25–500 Å. The analysis of the angular dependence of the resonance field H_0 allowed us to determine the fourfold cubic anisotropy constant K_1 and the effective magnetization value M_{eff}. It was found that both values decrease with decreasing L and approach a constant value below a certain thickness. A theory of FMR is outlined demonstrating that for the case of the dc magnetic field lying in a film plane, the anisotropy constant can be interpreted as a combination of a volume anisotropy contribution and a $1/L$-dependent contribution from the surface anisotropy up to the thickness $L \leqslant 10^3$ Å. This means that for the experimentally studied thickness range the films may be considered as "dynamically thin films" with respect to surface perturbations. Then the peculiar thickness dependence of the K_1 value can be explained assuming that the relaxation of the strain due to the mismatch between film and substrate extends to distances as far as 45 Å from the film-substrate interface. Since our SQUID measurements show that the saturation moment does not depend on the thickness, it is concluded that the thickness dependence of the effective magnetization M_{eff} is caused by a second-order uniaxial anisotropy arising mainly from the broken symmetry of the crystal field at surfaces and near the edges of interfacial dislocations.

I. INTRODUCTION

The magnetic anisotropies of thin films are determined to a large degree by surface or interface effects. A well known example of surface anisotropy is the Néel anisotropy,[1] which is caused by broken symmetry at the surface. Due to this effect, with decreasing the film thickness down to 1–10 atomic layers the magnetization of the film tends to be normal to the film plane. The interfacial anisotropy does exist not only in the out-of-plane direction, but can also arise within the plane of the film. For example, in single crystal $(1\bar{1}0)$ Fe films, grown on {110} W substrate the easy axis of magnetization is switched from [001] to [110] crystallographic axis below a critical film thickness.[2] This effect was ascribed to a competition between interface and bulk crystal anisotropies. The interface anisotropy may be influenced by the roughness and mosaicity of a substrate as well as due to perturbations of crystal field and band hybridization at the interface. Among different contributions to the magnetic anisotropies the interfacial effects due to the film-substrate mismatch may have a pronounced impact on the magnetic anisotropies of ultrathin films with thicknesses of several atomic layers[3] as well as of much thicker films.[4] The latter is due to the extension of the strain relaxation arising from the mismatch between film and substrate to distances up to 20–50 Å from the film-substrate interface.[5,6] Therefore in films with thicknesses above hundred angstroms the large number of atomic layers involved in the strained area makes this effect significantly stronger than the "pure" surface effect and its understanding becomes essential for thin film investigations in general.

In this paper we report on investigations extending our previous study[7] of the interfacial effects due to the film-substrate mismatch in iron films grown on magnesium oxide substrate. Iron gains much attention, because it is a widely used material in superlattices together with other nonmagnetic or even superconducting materials.[8,9] According to results of a model calculation of the Fe/MgO(001) interface by Li and Freeman[10] the MgO(001) forms a substrate with very weak electronic interactions for Fe thin films. This gives a hint that strain due to the mismatch between film and substrate will have primary impact on the magnetic anisotropy of iron films on MgO substrate. We performed ferromagnetic resonance (FMR) and superconducting quantum interference device (SQUID) measurements of iron films with thickness in the range 25–500 Å. It is well known[11] that the FMR technique is a sensitive tool for the study of the surface magnetic anisotropy problems. For the ultrathin films with thicknesses smaller than the so-called exchange length $\lambda_{\text{ex}} = (A/2\pi M^2)^{1/2}$ the anisotropy field measured by FMR can be interpreted as a combination of the volume anisotropy contribution and the $1/L$-dependent contribution from the surface anisotropy (A is the exchange stiffness constant and M is the saturation magnetization: $A = 2 \times 10^{-6}$ ergs/cm,

$M = 1700$ G, and $\lambda_{ex} \approx 50$ Å for iron at room temperature[11]). It has been reasoned however,[12] that for thicker films the anisotropy constant depends on the surface anisotropy contribution in a more complicated manner. Here we show theoretically that for the in-plane orientation of the dc magnetic field iron films may still be treated as "dynamically thin films" up to the thicknesses of 10^3 Å. Therefore magnetic parameters of the films measured by FMR were found to be averaged over the whole sample just similar to the case of ultrathin films with thickness $L < \lambda_{ex}$. In view of this the experimentally obtained thickness dependences of the fourfold cubic anisotropy constant K_1 and the effective magnetization value M_{eff} are explained assuming that the relaxation of strain due to the mismatch between film and substrate extends to large distances from the film-substrate interface.

This paper is organized as follows. In Sec. II we provide a brief outline of the sample preparation and characterization, and describe the details of FMR and SQUID measurements. Experimental results are presented in Sec. III, followed by their analysis in Sec. IV. We present a discussion of our results on the cubic anisotropy constants and effective magnetization in Sec. V. The main experimental and theoretical results are summarized in Sec. VI. In the Appendix we describe the calculation of the FMR absorption spectrum.

II. EXPERIMENT

A. Film preparation and characterization

Fe films in the thickness range from 25 to 500Å were grown by rf sputtering on high-quality MgO(001) substrates at 300 K. Pure Ar (99.999%) was used as a sputter gas at pressures of 5×10^{-3} mbar. The growth rate was controlled by a quartz crystal monitor and the rate of 0.1 Å/s has been found optimal to ensure a high quality of the grown iron films. The sample preparation and the growth conditions are described in more detail in our previous publications.[13] In order to prevent oxidation of the magnetic layers, the iron films were covered by a protective gold layer of 40 Å thickness.

The structural properties of all prepared films were studied by out-of-plane and in-plane x-ray scattering experiments. These data are presented in Ref. 13. Therefore only the main results will be stated here briefly. X-ray reflectivity measurements yielded interface and surface roughnesses, averaged over large distances of 4 to 6 Å , indicative for the high quality of the samples. The structural coherence length perpendicular to the film plane is of the order of the total film thickness and the out-of-plane mosaicity is about 0.8°. The epitaxial relation between bcc Fe(100) and fcc MgO(100) is the expected 45° epitaxy, i.e., the Fe[100] in-plane axis is parallel to the MgO[110] axis. The in-plane and out-of-plane lattice parameters of the Fe film appear to be roughly independent on the film thickness for thicknesses above 100 Å.

B. FMR measurements

FMR experiments were carried out at 9.4 GHz in a rectangular TE_{102} cavity and in the temperature range from 20 to 400 K. The angular dependences of the spectra were observed with both the dc magnetic field and the high frequency field lying in the film plane, but perpendicular to each other. The ϕ_H angles were measured in reference to the crystallographic Fe-[100]-in-plane axis of the films. The detected FMR signal corresponded to the field derivative of the absorbed microwave power. The resonance field H_o has been taken as the field midway between the field values corresponding to the absorption derivative extrema. The estimated uncertainty of the peak-to-peak linewidth ΔH_{pp} is of the order of 10% and thus the uncertainty of H_o is of the order of 0.1 ΔH_{pp}. The orientation accuracy of the magnetic field was better than 2°. The magnetic fields were calibrated by an NMR magnetometer.

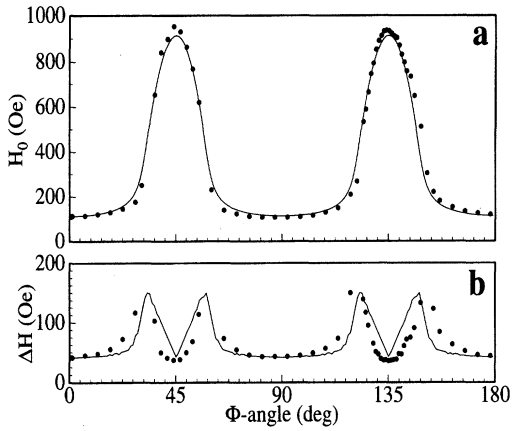

FIG. 1. In-plane angular dependence of the resonance field H_o (a) and of the linewidth ΔH_{pp} (b) for the sample of 250 Å thickness at $T = 355$ K. The solid line in (a) is the calculated resonance field assuming $4\pi M_{eff} = 19.0$ kG and $K_1 = 3.5 \times 10^5$ ergs/cm^3.

C. SQUID measurements

The magnetic moment measurements of the samples with thicknesses from 80 to 500 Å and in the temperature range from 4.2 to 300 K were performed using a SQUID magnetometer. The field dependences of the magnetic moments were measured in magnetic fields up to 5 kOe applied in the plane of the film. In order to correct the contribution of the substrate to the magnetic moment of the samples, the magnetic moments of the substrates were also measured separately after removing the magnetic films. Estimates show that such correction may cause not more than 10 % error of the obtained value of the magnetic moment of the film. Another source of error in determining the magnetic moments of the films are the interface and surface roughnesses. As pointed out above, the magnitude of the roughness is smaller than 6 Å. This can lead to an additional error of the order of 3% for a film of 100 Å thickness. Thus the total error in the determination of the saturation moment for the studied films is expected to be less than 13%.

III. EXPERIMENTAL RESULTS

FMR data on the angular dependences of the resonance field value H_o and of the linewidth ΔH_{pp} for the 250 Å thick sample at two different temperatures are shown in Fig. 1 and Fig. 2. For $T \geq 320$ K a single resonance line was observed.

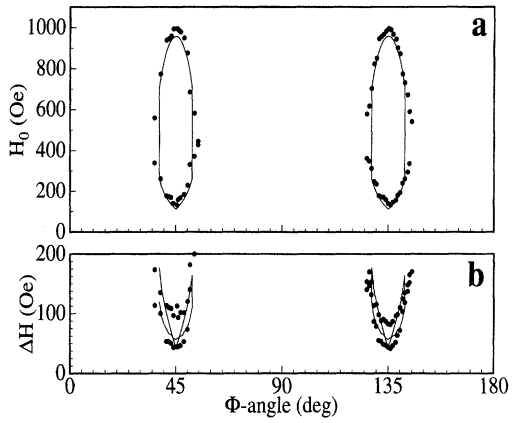

FIG. 2. In-plane angular dependence of the resonance field H_o (a) and of the linewidth ΔH_{pp} (b) for the sample of 250 Å thickness at $T=293$ K. The solid line in (a) is the calculated resonance field assuming $4\pi M_{\text{eff}} = 20.2$ kG and $K_1 = 4.1\times 10^5$ ergs/cm^3.

A fourfold anisotropy of the resonance field which is expected for cubic crystals and for the case of the dc magnetic field rotating in the Fe(001) plane is seen for this line. For temperatures below 300 K, two resonance lines were observed in the vicinity of the {110} axes of the film (Fig. 2). These lines disappeared at angles about 10 degrees away from these axes. A similar behavior of H_o was observed for the other samples studied, although at different temperatures: for example, the change of the type of the angular dependence occurs at lower temperatures ($T\sim$ 200 K) for the 100 Å thick sample and at higher temperatures ($T\sim$ 360 K) for the 500 Å thick sample. As it will be shown below the shape of the FMR spectrum as a function of ϕ depends on the relative saturation magnetization, on the magnetic anisotropy constant, and on the frequency at which the FMR measurements are performed.

For the samples with thickness $L\leqslant 40$ Å a main line exhibiting a very small fourfold in-plane anisotropy was observed together with an additional weak line showing a strong fourfold in-plane anisotropy. The intensity of the latter did not exceed 10% of the intensity of the main line.

The linewidth as a function of ϕ exhibits the largest value at the angles which correspond to a highest value of $|\partial H_0/\partial\phi|$. This is true for the case of a resonance line being only observable around the hard axis as well as for a continuous $H_o(\phi)$ behavior.

Figure 3 shows the typical results of SQUID measurements at $T=4.2$ K. At temperatures below 100 K the paramagnetic contribution to the magnetic moment of the sample caused by uncontrolled impurities in the substrate material becomes comparable to the ferromagnetic moment of the film. The field dependence of the magnetic moment of the film which was obtained by subtraction of the magnetic moment of the substrate from the total moment of the sample is also shown in this figure. The saturation moments extracted from these measurements for two temperatures are listed in Table I.

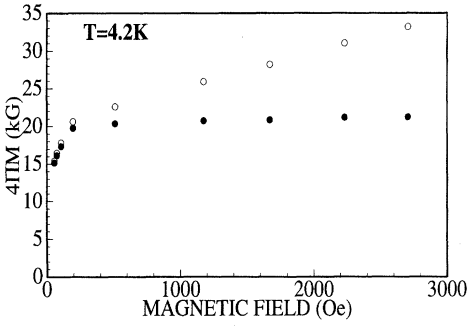

FIG. 3. The field dependences of the total magnetic moment value for the Fe/MgO sample with $L=80$ Å (open symbols), and of the magnetic moment of the film obtained by subtraction of the magnetic moment of the substrate (closed symbols).

IV. ANALYSIS

A. Resonance field

The FMR results are analyzed using a coordinate system in which the magnetization M of the film makes an angle θ with respect to the film normal (z direction) and an angle ϕ with respect to the x axis in the film plane (xy plane). The external magnetic field H is applied at an angle θ_H with respect to the film normal and an angle ϕ_H with respect to the x axis. We define the x axis to be parallel to the [100] axis of the Fe film. In our experiments θ_H was equal to $\pi/2$.

In general, ultrathin films of cubic materials grown along the [001] crystallographic axis have a tetragonal symmetry due to in-plane epitaxial strain and corresponding out-of-plane Poisson distortion. Therefore, the corresponding contribution to the free energy due to the crystal anisotropy contains (see, e.g., Ref. 11) the fourfold in-plane anisotropy constant which differs from the fourth-order constant for the perpendicular to the film plane direction. In addition, a nonzero second-order uniaxial anisotropy term appears due to the vertical lattice distortion and broken symmetry of crystal field acting on the interface atomic layer. The corresponding energy term has the form $F_u = -K_u\cos^2\theta$, where K_u may, in principle, depend on the film thickness. Since our experiments were performed in the in-plane geometry only, we will use the crystal anisotropy energy for cubic instead of tetragonal symmetry introducing an effective demagnetizing field

$$4\pi M_{\text{eff}} = 4\pi M - \frac{2K_u}{M}, \tag{1}$$

TABLE I. SQUID measurements data on the saturation magnetization.

L,Å	$4\pi M$, kG ($T=4.2$ K)	$4\pi M$, kG ($T=125$ K)
80	21.2	21.6
100	18.3	17.7
250	21.0	20.4
500	21.6	22.5
bulk (Ref. 15)	22.0	21.7

in order to account for the second-order perpendicular uniaxial anisotropy. Thus the total magnetic free energy density function appropriate for a (001)-oriented film is written in the form

$$F=-MH\sin\theta\cos(\phi-\phi_H)+2\pi M_{\rm eff}^2\cos^2\theta + \frac{1}{4}K_1(\sin^2 2\theta+\sin^4\theta\sin^2 2\phi). \quad (2)$$

Here K_1 is the fourth-order cubic anisotropy constant.

The equilibrium position of M is given by the zeros of the first angular derivatives of F. In our experimental situation the out-of-plane equilibrium angle is $\theta_0=\pi/2$, and the equilibrium in-plane angle ϕ_0 is given by solution of equation

$$H\sin(\phi_0-\phi_H)=-\frac{K_1}{2M}\sin(4\phi_0). \quad (3)$$

Using the general ferromagnetic resonance condition[14]

$$\omega=\frac{\gamma}{M\sin\theta}\left[\frac{\partial^2 E}{\partial\theta^2}\frac{\partial^2 E}{\partial\phi^2}-\left(\frac{\partial^2 E}{\partial\theta\partial\phi}\right)^2\right]^{1/2} \quad (4)$$

we obtain

$$\left(\frac{\omega}{\gamma}\right)^2=\left[H\cos(\phi_o-\phi_H)+4\pi M_{\rm eff}+\frac{K_1}{2M}[3+\cos(4\phi_o)]\right] \times\left[H\cos(\phi_o-\phi_H)+\frac{2K_1}{M}\cos(4\phi_o)\right]. \quad (5)$$

$\gamma=g\mu_B/\hbar$, and g is the spectroscopic g factor. The expression (5) together with the condition for equilibrium (3) determine the resonance field position H_o as a function of the angle ϕ_H, of the effective magnetization $4\pi M_{\rm eff}$, and of the anisotropy constant K_1. The analysis of Eqs. (3) and (5) shows that these equations have simultaneous solutions for the easy direction ([100] axis) only if $(2K_1/M)\leqslant(\omega/\gamma)^2/(4\pi M_{\rm eff})$ (assuming $4\pi M_{\rm eff}\gg|2K_1/M|$). In this case the FMR spectrum consists of a single line and the angular variation of H_0 is continuous, i.e., one can observe a single resonance line for any orientation of the external field in the film plane. In the opposite case, the resonance line disappears in the easy direction and there are two solutions in the vicinity of the hard axis. Equation (3) has the solution $\phi_0=\phi_H$ for easy ($\phi_H=0$) and hard ($\phi_H=\pi/4$) in-plane magnetic anisotropy axes. According to Eq. (5) for these directions and for the case when the resonance line is observed for any orientation of the external field we can obtain the resonance field value

$$H_0\simeq\left[\sqrt{Q^2+\left(\frac{\omega}{\gamma}\right)^2}-Q\right]\mp 2\frac{K_1}{M}, \quad (6)$$

where $Q=2\pi M_{\rm eff}+(3K_1/4M)$, and the minus and plus signs refer to the easy and hard directions, respectively. The accepted approximation $2\pi M_{\rm eff}\gg K_1/M$ is fulfilled in our case with a high degree of accuracy. Therefore, Eq. (6) gives the possibility to determine independently K_1 and $M_{\rm eff}$ values: the amplitude of the angular dependence of the resonance field is about $4K_1/M$ and the mean H_0 value (the term in brackets) is mainly determined by the effective moment

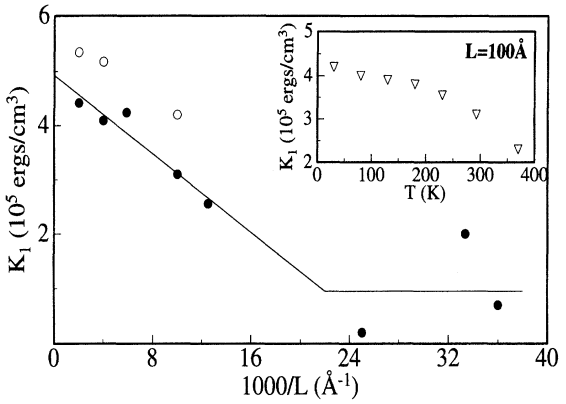

FIG. 4. The thickness dependences of the anisotropy constant K_1 at different temperatures. The solid line is the fit of the $T=293$ K data by Eq. (11) assuming $K_1^S=1.2\times10^5$ ergs/cm^3 and $\delta L=45$ Å. Inset: The temperature dependence of the K_1 value for the 100 Å thick sample.

value and by the g value. In order to fit the angular dependences of H_0 we used Eqs. (3) and (5) for numerical computations without any approximations. Typical fits for $g=2.09$ (Ref. 15) can be seen in Fig. 1(a) and 2(a). They are in good agreement with the experimental data. Figures 4 and 5 show the thickness dependences of K_1 and $4\pi M_{\rm eff}$ values at two different temperatures. The typical temperature dependences of these values are also shown in Figs. 4 and 5. The present data on the thickness dependence of K_1 are in good agreement with those obtained earlier from magneto-optic Kerr effect measurements.[16]

The peculiar angular dependence of H_o shown in Fig. 2 has already been observed[17] for epitaxially grown Fe(100) thin films on Ag/GaAs substrate. The values of $K_1=4.1\times10^5$ ergs/cm^3 and $4\pi M_{\rm eff}=19.8$ kG deduced from the fitting of our room temperature data for the 250 Å thick sample are in good agreement with the values $K_1=4.9\times10^5$ ergs/cm^3 and $4\pi M=20.7$ kG obtained earlier[17] for a 200 Å thick Fe film.

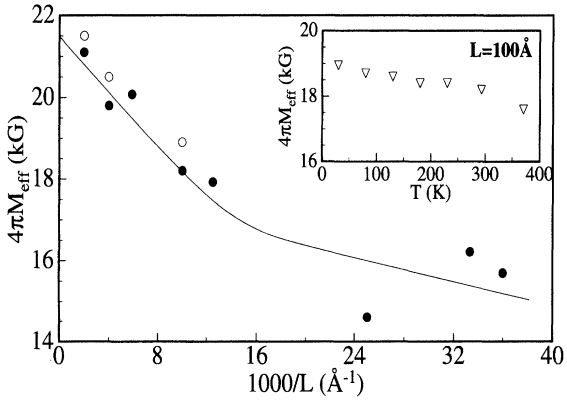

FIG. 5. The thickness dependences of the $4\pi M_{\rm eff}$ value at different temperatures. The solid line is a guide for eyes for the $T=293$ K data. Inset: The temperature dependence of the $4\pi M_{\rm eff}$ value for the 100 Å thick sample.

B. FMR linewidth

It is known[11] that the FMR linewidth is mainly determined by two mechanisms: the intrinsic damping and the magnetic inhomogeneities of the sample. In order to extract the intrinsic contribution to the FMR linewidth it is necessary (see, e.g., Ref. 18 and references therein) to know the frequency dependence of the FMR linewidth. In this study such measurements were not performed. Nevertheless some estimates can be presented. According to Suhl[14] the intrinsic contribution to the linewidth can be obtained as

$$\Delta H_{pp}^{\text{int}}(\phi)=\frac{2}{\sqrt{3}}\frac{1}{|\partial\omega/\partial H|}\frac{G}{M^2}\left(\frac{\partial^2 F}{\partial\theta^2}+\frac{1}{\sin^2\theta}\frac{\partial^2 F}{\partial\phi^2}\right)$$

$$\approx\frac{2}{\sqrt{3}}\frac{G}{\gamma^2 M}\frac{\omega}{\cos(\phi_0-\phi_H)}, \tag{7}$$

where G is the Gilbert damping parameter. This contribution passes over the minimum at principal magnetic directions and it has a maximum value at the points where the magnetization orientation undergoes strong changes.

The inhomogeneous contribution to the FMR linewidth may arise due to the lattice defects ΔH_{pp}^{D} and due to the mosaicity of the studied samples. The first one is independent on ϕ, the latter depends on it. The mosaicity $\Delta\tilde{\phi}$ of the crystallographic axes will lead[19] to a contribution of the order of $|\partial H_0/\partial\phi|\cdot\Delta\tilde{\phi}$. Thus the angular dependence of this contribution is exactly the same as it has been observed experimentally [Figs. 1(b) and 2(b)]. Now the total FMR linewidth may be written as

$$\Delta H_{pp}^{\text{total}}(\phi)\simeq\Delta H_{pp}^{D}+\Delta H_{pp}^{\text{int}}(\phi)+\left|\frac{\partial H_0}{\partial\phi}\right|\Delta\tilde{\phi}. \tag{8}$$

Taking $\omega=6\times10^{10}$ rad/s and experimentally measured[18] $G=6\times10^{7}$ rad/s we obtained the minimum value of $\Delta H_{pp}^{\text{int}}\approx6.8$ Oe and the maximum value of $\Delta H_{pp}^{\text{int}}\approx10$ Oe. Hence the intrinsic contribution to the observed linewidth is not enough to explain the angular variations of the total linewidth. The fitting of the angular dependences of the linewidth by Eq. (8) [see Figs. 1(b) and 2(b)] gave $\Delta H_{pp}^{D}=34$ Oe and $\Delta\tilde{\phi}=1.5°$. The obtained $\Delta\tilde{\phi}$ is comparable with the measured value of mosaicity (see Sec. II).

V. DISCUSSION

A. Cubic anisotropy constants

The experimentally determined in-plane fourfold anisotropy constant in our samples depends strongly on the sample thickness. At $T=300$ K for the thickness range from 500 to 80 Å this dependence can be described by the following expression:

$$\frac{2K_1}{M}=\left(0.58-\frac{14.6}{d}\right)\ \text{kOe}, \tag{9}$$

where d is the film thickness in monolayers (ML) [$d=L/1.433$ Å for bcc Fe(001)]. Qualitatively this dependence resembles that obtained by Heinrich *et al.*[20] for Fe(001) films on Ag substrate. The constant term in Eq. (9) is close to the anisotropy field value for bulk samples.[15] The $1/d$ term has been supposed earlier[20] to originate from a surface fourfold anisotropy term. In this case the negative sign of the d dependent contribution indicates that the surface anisotropy energy has its easy axis parallel to the {110} crystallographic directions. This means that there is a certain thickness value at which the observed anisotropy constant K_1 changes its sign. If we suppose that in our case the thickness dependence of K_1 has the same origin, then in accordance with Eq. (9) the change of the sign of anisotropy constant should occur at $L=36$ Å. However, as it can be seen from Fig. 4 this does not take place.

The coefficient of the $1/d$ term for Fe(001) films on silver substrates was obtained[20] to be equal to 2.5. If we take the ratio of the $1/d$ term coefficients for Fe/MgO and Fe/Ag and compare it with the ratio of the epitaxial mismatch $\eta=(a_d-a_s)/a_s$ between the substrate lattice parameter a_s and the deposit parameter a_d for these systems ($\eta=-4\times10^{-2}$ and -0.8×10^{-2}, respectively) we see that these two ratios are very close to each other. Most likely this indicates that in both cases the reason for the thickness dependence of the K_1 value arises from the mismatch at the film-substrate interface.

It is known from grazing incidence x-ray scattering experiments[5,6] that in case of large mismatch values, the strain relaxation may extend to large distances from the film-substrate interface. The data obtained in Ref. 6 indicate an initial island growth up to the thickness of 10 ML's of the iron films on MgO(001) substrate at $T=$ 360 K. Upon the subsequent increase of the film thickness, the islands containing initially a small strain, coalesce with each other. Just at this moment the maximum value of strain is observed. Then the value of strain starts to decrease and at the thickness of 20–25 ML's it becomes an order of half of its maximum value. The strain located near the interface area can change the magnetic anisotropy constant of this border layer via the magnetostriction. The small value of the structural coherence length in the border layer can also lead to a decrease of the in-plane magnetic anisotropy.

In order to establish a physical origin for the $1/d$ term in the anisotropy field we performed calculations of the FMR absorption spectrum. These calculations are outlined in the Appendix. The analysis given in the Appendix shows that due to the existence of the long wavelength magnetization transfer process, the source of the interface anisotropy located at the boundary layer of finite thickness $\delta L\ll L$ near the interface will look as a "true" surface anisotropy of much larger value, spread over the whole thickness L of the film. Nevertheless, it is also evident that as the film thickness L approaches the thickness δL of the boundary layer, the $1/d$ dependence of anisotropy field should saturate at the value characterizing the averaged anisotropy field within δL. Now the reason for the enhanced scattering of the experimental points in Fig. 4 at small film thicknesses also becomes clear. It is natural to assume that the degree of the lattice distortion of the boundary layer depends on a set of uncontrolled factors. As the contribution of the boundary layer with an uncertain K_1^S value increases with decreasing film thickness, the uncertainty in the K_1 parameter of the film increases as well. The additional weak resonance line showing a strong four-

fold in-plane anisotropy which was observed for the samples with thicknesses $L \leq 40$ Å can be attributed to the remaining islands which did not yet coalesce with the main part of the films.

Let us stress here, that we applied the definition of the surface anisotropy as $K_1^S a_0$ in the boundary conditions (A2) implying the interpretation of K_1^S parameter, as the volume characteristics of the magnetic anisotropy of the border layer. As pointed out above, we suppose that the change of the magnetic anisotropy parameter of the border layer can be caused by the strain arising due to the mismatch at the film-substrate interface. Generally, in order to describe the thickness dependence of the magnetic anisotropy it is necessary to know the distribution of strain in the space near the interface. However, the explicit form of this distribution can not be calculated unambiguously. Let us assume the simplest step-like distribution of the anisotropy constant near the interface, i.e.,

$$K(z)=\begin{cases} K_1^V & \text{if } 0 \leq z \leq L-\delta L \\ K_1^S & \text{if } L-\delta L < z \leq L. \end{cases} \tag{10}$$

Then the total anisotropy averaged over the film thickness can be written as

$$K_1=\frac{1}{L}\int_0^L K(z)dz=\begin{cases} K_1^V-(\delta L/L)(K_1^V-K_1^S) & \text{if } L>\delta L \\ K_1^S & \text{if } L \leq \delta L. \end{cases} \tag{11}$$

Until $L > \delta L$, the expression (11) provides a $1/L$- (or $1/d$)-depending contribution to the total anisotropy field. As the value of L- becomes equal to δL, K_1 becomes constant, causing deviations from the initial $1/d$ law (9) and preventing the sign change of the anisotropy field. Obviously, any smooth distribution of K_1^S values (for example, an exponential decay) will produce a similar behavior, but with continuous transition from the $1/L$ dependence of K_1 to a saturation at small thicknesses.

By fitting of our experimental data on the thickness dependence of the anisotropy field to Eq. (11) we obtain the parameters $K_1^S \approx 1.2\times 10^5$ ergs/cm^3 and $\delta L \approx 45$ Å. Using the experimental data on the stress value dependence on the film thickness,[6] we we can estimate the depth of the boundary layer to be 20–25 ML ($\sim$ 30–40 Å) which agrees well with our results. Certainly, the above fitting as well as the obtained K_1^S and δL parameters can be considered as rather rough approximations, because the shape of the thickness dependence and the K_1^S value strongly depends on local variation of the magnetic anisotropy constant.

An additional support of the suggested model was obtained by our FMR measurements of the 120, 250, and 500 Å thick samples which were grown on MgO(001) substrates at 470 K. The thickness dependence of the K_1 value for this set of samples can be described by the empirical expression

$$\frac{2K_1}{M}=\left(0.59-\frac{8.3}{d}\right) \text{ kOe}. \tag{12}$$

Comparison of the coefficient of the $1/d$ term in formulas (9) and (12) shows that the average value of strain in the samples grown at 470 K is smaller than in those prepared at room temperature. It seems feasible that the relaxation of strain in the samples grown at higher temperatures occurs at smaller distances from the film-substrate interface.

B. Effective magnetization

Results of our SQUID measurements (see Table I) show that the value of the saturation moment M seems to be independent on the film thickness. Therefore the obtained dependence of the effective magnetization is most likely associated with the second-order uniaxial anisotropy [see Eq. (1)]. Such anisotropy can arise due to the magnetostriction and due to perpendicular Néel anisotropy.[1]

Thin films are usually strained to some degree and therefore are affected by the magnetoelasticity. Vertical lattice distortion which is due to the epitaxial mismatch, can result in a perpendicular uniaxial anisotropy field[20]:

$$\frac{2K_u^{\text{mag.el.}}}{M}=-\frac{2B_1}{M}(\varepsilon_\perp-\varepsilon_{||}), \tag{13}$$

where $(\varepsilon_\perp-\varepsilon_{||})$ is the value of tetragonal strain and B_1 is the corresponding magnetoelastic coefficient[21]: $B_1=-2.9\times 10^7$ ergs/cm^3 for Fe. The value of strain $(\varepsilon_\perp-\varepsilon_{||})$ can be estimated from the data on the in-plane lattice parameter of iron films on MgO substrate measured down to monolayer level.[6] For the $L=100$ Å film we obtain $\varepsilon_{||}=1.3\times 10^{-2}$. Supposing that the tetragonal distortion of the Fe layer is of purely elastic origin ($\varepsilon_\perp=-\varepsilon_{||}2C_{12}/C_{11}$, where the C_{ij} are the elastic moduli: $C_{11}=2.41\times 10^{12}$ ergs/cm^3, $C_{12}=1.46\times 10^{12}$ ergs/cm^3 for iron[21]) we can find $(\varepsilon_\perp-\varepsilon_{||})=-2.9\times 10^{-2}$. Then the magnetoelastic contribution becomes

$$\frac{2K_u^{\text{mag.el.}}}{M}\approx -1 \text{ kOe}. \tag{14}$$

Thus this contribution to the uniaxial anisotropy causes an enhancement of the effective magnetization value which is in contradiction with our experimental results.

The next reason for the renormalization of saturation magnetization seen in FMR is the axial crystal field, generated by the surface even for films with cubic structure due to the low symmetry local environment at a surface.[1] Adding to (2) the energy of the axial symmetry

$$\delta F=(K_S/d)\cos^2\theta, \tag{15}$$

and taking into account the results of our calculations of the FMR line shape which show that for our films the surface contribution to the anisotropy constant can be written as the $1/d$-dependent term, we obtain

$$\frac{2K_u^N}{M}=\frac{2K_S}{dM}. \tag{16}$$

A microscopic theory for axial crystal fields at the surface does not exist, but it is reasonable to expect that the axial crystal field constant K_S scales as the magnetoelastic constant B_1 since both of them have the same microscopic origin.[1,22] Indeed, one can think that the magnetoelastic energy is mainly determined by an axial crystal field contribution to the orbit-lattice interaction. Therefore one can use the

value of the orbit-lattice (magnetoelastic) coupling constant B_1 as a rough estimate of the axial crystal field acting on the surface magnetic ions. Assuming $K_S = B_1$ one can obtain

$$\frac{2K_u^N}{M} = (34/d) \text{ kOe}, \tag{17}$$

obtaining $(2K_u^N/M) = 0.5$ kOe for $d = 70$ ML ($L = 100$ Å) sample as an example. This value should be compared with the experimentally observed $(2K_u/M) = 3$ kOe. Therefore the sign of this contribution is correct, but its magnitude is too small to account for the observed reduction of magnetization. It is interesting to note that the value of surface contribution (17) is very close to that observed experimentally for Fe/Ag films.[20] One may think that Néel anisotropy contribution dominates for such samples because the mismatch for the Fe/Ag interface is five times smaller than in the case of Fe on MgO substrate. It should also be noted that for the set of samples grown at 470 K the reduction of $4\pi M_{\text{eff}}$ does not exceed the value predicted by the Néel mechanism [see Eq. (17)]. As to the samples grown at room temperature, the above estimates show that a simple Néel picture cannot explain the large uniaxial perpendicular anisotropy observed for our samples. The analysis of the data shown in Figs. 4 and 5 allows us to conclude that the thickness dependences of the K_1 and K_u values are quite similar: both values are strongly changed with decreasing L and approach a constant value below a certain thickness. This indicates that the thickness dependence of both parameters has a common origin, which is the strain arising due to the mismatch at the film-substrate interface. As shown above [see Eq. (14)] the strain gives a contribution to the uniaxial anisotropy with a sign opposite to that observed experimentally. It should be noted, however, that the lattice mismatch may not completely be taken up by strain and that dislocations are generated at the interface.[23] In our case this is manifested by the data on the in-plane lattice parameters of iron films on MgO substrate[6]: the maximum value of the in-plane strain $\varepsilon_{||}$ is two times smaller than the epitaxial mismatch η. At the dislocation edge the symmetry of the crystal field is broken just as if it would be a surface. It is difficult to estimate the magnitude of this contribution to the perpendicular uniaxial anisotropy. However, it is obvious that the dislocation density as well as the number of atomic planes with broken symmetry are extremely high ensuring a fast relaxation of the lattice mismatch at distances of the order of 40–50 Å. We can therefore conclude that the Néel mechanism providing the correct sign of K_u may be considerably enhanced by interfacial dislocations.

VI. SUMMARY

In conclusion, FMR measurements of rf sputtered Fe films on MgO(001) substrates have been performed in a wide temperature range. Two different types of angular dependences of the resonance field value have been observed at various temperatures. Our analysis shows that the realization of one or another type of angular dependence is determined by the relation between the effective magnetization $4\pi M_{\text{eff}}$ and the anisotropy constant K_1. By numerical fitting of the angular dependent FMR measurements we determined independently the anisotropy constant K_1 and the effective magnetization value M_{eff}. We have observed a thickness dependences of K_1 and $4\pi M_{\text{eff}}$ and suggested that it may be caused by epitaxial strain extended to a large distance of the order of 45 Å from the film-substrate interface. This result is based on our calculation of the FMR line shape which shows that in parallel orientation of the dc magnetic film relative to the film plane the measured anisotropy constant can be represented as a combination of the volume anisotropy and $1/d$-dependent part from the surface anisotropy in the thickness range studied experimentally. We argue that the observed decrease of the $4\pi M_{\text{eff}}$ value in comparison with the bulk saturation magnetization together with its L dependence may be caused by interface contributions to the out-of-plane uniaxial anisotropy competing with the shape anisotropy.

This work is supported by the Deutsche Forschungsgemeinschaft (DFG-ZA161/6-1).

APPENDIX

In order to clarify how the change of the magnetic anisotropy constant of the extended border layer near the film-substrate interface influences the magnetic parameters measured by FMR we performed calculations of the FMR line shape. We solved the boundary problem for the system of surface/magnetic film/interface/dielectric substrate, subjected to action of the dc and the high frequency magnetic fields for the experimental geometry described above.

We assume the cubic symmetry of the volume anisotropy energy to be present in our magnetic layer with fourfold anisotropy constant K_1^V. Then we suppose the surface anisotropy of cubic symmetry to be located within a very thin interface region between film and substrate. Therefore we neglect temporarily the thickness of interface area. We describe the dynamics of nonequilibrium magnetization induced by microwave field by Landau-Lifshitz equations[24] with boundary conditions just neglecting the surface anisotropy torque, acting on the film magnetization at the interface. In line with the discussion in Ref. 25, linearized equations, written for the circular components of magnetizations $m_\pm = m_y \pm i m_z$, are

$$\begin{aligned} &D\frac{\partial^2 m_+}{\partial z^2} + \left(\frac{\omega}{\gamma} - H - 2\pi M - H_1\right) m_+ + (2\pi M + H_2) m_- \\ &\quad = -hM \\ &D\frac{\partial^2 m_-}{\partial z^2} - \left(\frac{\omega}{\gamma} + H + 2\pi M + H_1\right) m_- + (2\pi M + H_2) m_+ \\ &\quad = -hM, \end{aligned} \tag{A1}$$

where $D = 2A/M$, $H_1 = 2K_1^V/M$, $H_2 = 0$ for the case of easy direction, and $H_1 = -K_1^V/M$, $H_2 = 3K_1^V/M$ for the hard direction of M and h is the microwave field amplitude. The boundary conditions for the magnetization components can be obtained in the form

$$D\frac{\partial m_\pm}{\partial z}\bigg|_{z=L} = \frac{2(K_1^V - K_1^S)a_0}{M} m_\pm, \quad D\frac{\partial m_\pm}{\partial z}\bigg|_{z=0} = 0; \tag{A2}$$

where a_0 is the interlayer spacing and K_1^S is the surface four-fold anisotropy constant per volume unit. The eddy current problem is not important for our films, because the skin-depth is larger than the actual films thickness. We solve Eqs. (A1) satisfying them and boundary con-ditions (A2) by the general solution

$$m_{\pm}(z)=m_{\pm}^0+A_{\pm}\cosh(k_1 z)+B_{\pm}\cosh(k_2 z). \quad \text{(A3)}$$

The quantities entering in the solution appeared to be as follows:

$$k_{1,2}=\frac{1}{\sqrt{D}}\sqrt{H+(2K_1^V/M)+2\pi M\pm\sqrt{(\omega/\gamma)^2+(2\pi M)^2}}, \quad \text{(A4)}$$

$$m_{\pm}^0=\mp Mh\gamma\frac{\omega\pm\gamma(H+4\pi M)}{\omega^2-\omega_0^2}, \quad \text{(A5)}$$

$$A_{\pm}=\frac{\lambda}{Dk_1\sinh(k_1L)+\lambda\cosh(k_1L)}\frac{\pi M}{\sqrt{(\omega/\gamma)^2+(2\pi M)^2}}\left(m_{\mp}^0\mp m_{\pm}^0\frac{2\pi M}{b_{\pm}}\right), \quad \text{(A6)}$$

$$B_{\pm}=\frac{\lambda}{Dk_2\sinh(k_2L)+\lambda\cosh(k_2L)}\frac{\pi M}{\sqrt{(\omega/\gamma)^2+(2\pi M)^2}}\left(m_{\mp}^0\mp m_{\pm}^0\frac{2\pi M}{b_{\mp}}\right), \quad \text{(A7)}$$

where $\lambda^S=K_1^S a_0/A$, $b_{\pm}=(\omega/\gamma)\pm\sqrt{(\omega/\gamma)^2+(2\pi M)^2}$, $(\omega_0/\gamma)^2=(H+2K_1^V/M)(H+2K_1^V/M+4\pi M)$. The homogeneous FMR linewidth δ is introduced by assuming $(\omega/\gamma)\to\omega/\gamma+i\delta$ in the above formulas. Taking into account the homogeneity of microwave field in the film, we integrate the solution (A3) over the film thickness thus obtaining the total response of ferromagnetic film on microwave excitation as

$$P(H)=-(\gamma Mh^2)\mathrm{Im}\left[\frac{2\omega}{\omega^2-\omega_0^2}\left(1-\frac{\lambda^S}{k_2L}\frac{1}{k_2+\lambda^S\coth(k_2L)}\frac{k_1^2}{k_1^2-k_2^2}+\frac{\lambda^S}{k_1L}\frac{1}{k_1+\lambda^S\coth(k_1L)}\frac{k_2^2}{k_1^2-k_2^2}\right)\right]. \quad \text{(A8)}$$

Direct inspection of Eq. (A8) shows that there exist two distinct scales for the propagation of dynamic magnetization which are determined by $k_1^{-1}\approx(A/2\pi M^2)^{1/2}$ and by $k_2^{-1}\approx[Ad/(K_1^V-K_1^S)]^{1/2}$. The first value is the usual exchange length λ_{ex} (see Introduction) and we shall call a corresponding short range mode—"exchange mode." The spatial scale of the second mode shows how deep the virtual spin waves carry the perturbation introduced by the surface. The thickness dependence of this scale is due to the dependence of spin-wave energy on the film thickness. The k_2^{-1} value increases upon increasing the film thickness L, but it is limited by the homogeneous FMR linewidth δ, for example. If one assumes that $|2(K_1^V-K_1^S)/Md|\ll\delta$, then the k_2^{-1} value can be estimated as $|k_2^{-1}|\approx(4\pi A\gamma/\omega_0\delta)^{1/2}\approx 10^3$ Å for our experimental situation $\delta\approx 50$ Oe. Actually $k_2^{-1}\sim 10^3$ Å $\gg\lambda_{ex}$ determines the penetration depth of the surface perturbation into the film. Hence this "surface induced mode" appears to be slowly varying in the space.

The intensities of the "surface induced" and "exchange" modes are represented by the first, second, and last terms in the square brackets of the expression (A8) for the total response, respectively. The analysis of corresponding expressions shows that the contribution of the exchange mode [last term in (A8)] is small already due to the smallness of the ratio $k_2^2/k_1^2\approx[2(K_1^V-K_1^S)/dM]/4\pi M\ll 1$ for parameters of our experiment. Approximate analysis and the computer simulation of the FMR spectra according to the explicit expression (A8) for $P(H)$ revealed that the contribution of the last term is negligibly small in our experimental situation (the film thickness ranges from 25 to 500 Å and magnetic field sweep varies from 0 to 1000 Oe). That is why only the surface induced mode should be observed in our experiments. Assuming $k_2L\ll 1$, from the poles of absorbed power (A8) we obtain the explicit resonance condition for films with easy direction of magnetization, subjected to surface anisotropy as

$$\left(\frac{\omega}{\gamma}\right)^2=\left(H+\frac{2K_1^V}{M}+\frac{2K_1^S}{dM}+4\pi M\right)\left(H+\frac{2K_1^V}{M}+\frac{2K_1^S}{dM}\right). \quad \text{(A9)}$$

The solution (A9) is just the same result which we can obtain considering the ultrathin film with microwave field and magnetizations $m_{\pm}$ being uniform across the film thickness.[12,25] Our analysis shows that the condition $|k_3L|\ll 1$ of Rado,[12] which is equivalent to our $|k_1L|\ll 1$, is redundant for the in-plane geometry of the experiment. Until the skin depth is much greater than the film thickness L, the short-scaled exchange mode does not couple with the homogeneous microwave field and produces only the low-intensity response with respect to slow varying surface mode.

[1] L. Néel, C. R. Acad. Sci. **237**, 1623 (1953).
[2] U. Gradmann, J. Korecki, and G. Waller, Appl. Phys. A **39**, 101 (1986).
[3] C. Chappert and P. Bruno, J. Appl. Phys. **64**, 5736 (1988).
[4] J. J. Krebs, F. J. Rachford, P. Lubitz, and G. A. Prinz, J. Appl. Phys. **53**, 8058 (1982).
[5] B. M. Clemens, R. Osgood, A. P. Payne, B. M. Larison, S. Brennan, R. L. White, and W. D. Nix, J. Magn. Magn. Mater. **121**, 37 (1993).
[6] B. M. Lairson, A. P. Payne, S. Brennan, N. M. Rensing, B. J. Daniels, and B. M. Clemens (unpublished).
[7] Yu.V. Goryunov, G. G. Khaliullin, I. A. Garifullin, L. R. Tagirov, F. Schreiber, P. Bödeker, K. Bröhl, Ch. Morawe, Th. Mühge, and H. Zabel, J. Appl. Phys. **76**, 6096 (1994).
[8] K. Kawaguchi and M. Sohma, Phys. Rev. B **46**, 14 722 (1992).
[9] J. E. Mattson, C. H. Sowers, A. Berger, and S. D. Bader, Phys. Rev. Lett. **68**, 3252 (1992).
[10] C. Li and A. J. Freeman, Phys. Rev. B **43**, 780 (1991).
[11] B. Heinrich and J.F. Cochran, Adv. Phys. **42**, 523 (1993).
[12] G. T. Rado, Phys. Rev. B **26**, 295 (1982); **32**, 6061 (1985); J. Appl. Phys. **61**, 4262 (1987).
[13] Th. Mühge, A. Stierle, N. Metoki, U. Pietsch, and H. Zabel, Appl. Phys. A **59**, 659 (1994).
[14] H. Suhl, Phys. Rev. **97**, 555 (1955).
[15] *Numerical Data and Functional Relationships in Science and Technology*, Landolt-Börnstein, New Series, Vol. III/19a (Springer, Heidelberg, 1986).
[16] N. Metoki, M. Hofelich, Th. Zeidler, Th. Mühge, Ch. Morawe, and H. Zabel, J. Magn. Magn. Mater. **121**, 137 (1993).
[17] E. C. da Silva, R. Meckenstock, O. von Geisau, R. Kordecki, J. Pelzl, J. A. Wolf, and P. Grünberg, J. Magn. Magn. Mater. **121**, 528 (1993).
[18] F. Schreiber, J. Pflaum, Z. Frait, Th. Mühge, and J. Pelzl, Solid State Commun. **93**, 965 (1995).
[19] C. Chappert, K. Le Dang, P. Beauvillian, H. Hurdequint, and D. Renard, Phys. Rev. B **34**, 3192 (1986).
[20] B. Heinrich, Z. Celinski, J. F. Cochran, A. S. Arrott, and K. Myrtle, J. Appl. Phys. **70**, 5769 (1991).
[21] C. Kittel and J. K. Galt, in *Solid State Physics*, edited by H. Ehrenreich, F. Seitz, and D. Turnbull (Academic, New York, 1956), Vol. 3, p. 439.
[22] G. G. Khaliullin and S. V. Buzukin, J. Phys. Condens. Matter **2**, 577 (1990).
[23] F. C. Frank and J. H. van der Merve, Proc. R. Soc. London Ser. A **198**, 216 (1949).
[24] L. D. Landau and E. M. Lifshitz, Phys. Z. Sowjetunion **8**, 153 (1935).
[25] J. F. Cochran, B. Heinrich, and A. S. Arrott, Phys. Rev. B **34**, 7788 (1986).